COMPDYN 2013
4th ECCOMAS Thematic Conference on
Computational Methods in Structural Dynamics and Earthquake Engineering
M. Papadrakakis, V. Papadopoulos, V. Plevris (eds.)
Kos Island, Greece, 12–14 June 2013

INFLUENCE OF THE LOADING RATE ON THE AXIAL COMPRESSIVE BEHAVIOR OF CONCRETE SPECIMENS CONFINED WITH SRG JACKETS

Georgia E. Thermou[1], Konstantinos Katakalos[1], and George Manos[1]

[1] Aristotle University of Thessaloniki
Dept. of Civil Engineering, 54124, Thessaloniki, Greece
gthermou@civil.auth.gr; kkatakal@civil.auth.gr; gcmanos@civil.auth.gr

Keywords: Retrofit, Strengthening, Jackets, Steel reinforcement, Axial compression, Loading rate

Abstract. *In the present paper, an experimental study was carried out where the main objective was to investigate the favorable confinement characteristics of steel reinforced grout (SRG) jackets on the compressive behavior of unreinforced concrete prisms under monotonic and cyclic axial loading. SRG jackets were made by applying steel fiber reinforced fabrics of reduced density combined with cementitious grout that serves as the connecting matrix. For this purpose, one layer of the novel jacketing system was applied to a number of unreinforced concrete prismatic specimens constructed for a moderate concrete cylindrical compressive strength of 25 MPa. The parameters of this investigation were: a) the density of the fabric used in the steel reinforced concrete jackets and b) the rate of axial loading. The density of the fabric was either medium (2 cords/cm) or relatively low (1 cord/cm). The specimens were subjected to monotonic concentric uni-axial compression load applied either in a slow rate reaching the maximum load in 400 secs or at a axial load rate ten times faster. Both the slow rate load and the fast rate load were applied in the following manner. Initially, approximately 50% of the maximum load was reached in 3 load-unload cycles that were followed by 3 load-unload cycles at approximately 75% of the maximum load before the specimen reached the maximum load and failure at a final loading cycle. The experimental sequence was carried out at the Laboratory of Strength of Materials and Structures of Aristotle University of Thessaloniki. The magnitude of the maximum load reached, as well as the mode of failure attained at the end of each loading sequence was monitored. From the obtained results, the influence of the loading rate on the ultimate compressive load and on the mode of failure in relation to the SRG jacket characteristics was studied. The whole effort intended to examine the effect on the response behavior of SRG jacketed specimens when axial load is dynamic in nature.*

1 INTRODUCTION

Reinforced concrete (RC) structures built according to older generation of codes present deficiencies related to structural integrity issues. Retrofitting is deemed necessary in order for this category of structures to survive future earthquake events by avoiding premature failure modes. When the retrofit strategy requires local intervention measures (at member level) to be taken or when the objective is the enhancement of the ductility level, then one of the most widely applied methods is wrapping with composite fabrics (carbon, glass or aramid). Although fiber reinforced polymer (FRP) jacketing is considered an efficient intervention method combining many advantages (no change in the geometry, fast in application, high-strength-to-weight ratio, corrosion resistance), issues related mainly to the high cost (due to the use of epoxy resins) and poor behavior of resins at high temperatures have led the research community to the investigation of new materials that will keep the easiness in application of the method (e.g. FRM [1], TRM [2]).

Within this framework, the last decade a new material has been introduced, the steel reinforced fabric combined with either polymer (SRP) or grout (SRG). This type of fabric consists of high strength steel cords embedded in epoxy resin or grout matrix. Most of the applications concern the use of SRP as externally bonded longitudinal reinforcement in flexural members [e.g. [3]-[13]]. The use of the steel reinforced fabric as a jacketing device was investigated experimentally to predamaged cantilever specimens of old type detailing for the first time in 2007 by Thermou and Pantazopoulou [14]. The proposed jacketing system comprised steel fiber reinforced fabrics of reduced density (this was required in order to improve impregnation of the metallic fibers in the intended matrix but also to reduce axial stiffness of the metallic fabric to the level of a carbon sheet) combined with cementitious grout that served as the connecting matrix. Recently, El-Hasha and Mashrik [15], El-Hacha and Abdelrahman [16] investigated experimentally the confinement effectiveness of resin impregnated high density steel fibre reinforced fabric (SRP) jackets applied to both cylindrical and prismatic specimens.

The SRG jacketing system proposed by Thermou and Pantazopoulou [14] was implemented in a large number of cylindrical specimens subjected to axial monotonic compression [17]. The results have shown that both strength and deformability were improved substantially for a single layer of jacket of medium to low density (The gain in compressive strength ranged between 47% and 84%, whereas the gain in ultimate strain ranged between 166% and 366%). Based on these promising results, the objective was to investigate further the potential of the SRG jackets, this time by applying the proposed retrofit scheme on prismatic specimens of square cross section subjected to both monotonic and cyclic axial compression. Despite the adverse effect of the edge sharpness increase on the confinement effectiveness, it was decided to keep a zero corner radius in order to simplify construction. Moreover, the nature of the loading was a parameter of study in order to observe the influence of the loading rate on the effectiveness of the SRG jackets.

An experimental study was carried out where the main objective was to investigate the effectiveness of SRG jackets on prismatic specimens with sharp edges subjected to both slow-rate and fast-rate axial compression up to failure. The slow-rate compression was applied in a monotonic way whereas a small number of cycles of load-unload were used in the fast-rate compression. Tests parameters were the density of the steel reinforced fabric and the nature of loading. The results have shown the SRG jacketing schemes tested herein provided a higher compressive strength compared to their unconfined counterparts. The role of the type of loading was revealed. The fast rate loading simulating dynamic loading in nature had a detri-

mental effect on the response of both unconfined and confined concrete prisms, rendering in some cases the applied confining measure ineffective.

2 CONFINEMENT OF UNREINFORCED CONCRETE PRISMATIC MEMBERS WRAPPED WITH COMPOSITE FABRICS

2.1 Edge sharpness impact on the axial compressive strength

The shape of the cross section influences in a determinant way the effectiveness of composite fabric jackets in increasing both strength and ductility of unconfined plain concrete. Experimental evidence has shown that as the edge sharpness of non-circular cross sections increases the composite wraps become less efficient [18]. This is explained by the fact that the confining internal lateral pressure is not uniformly distributed over the rectangular cross and instead confined and unconfined regions are developed (Fig. 1). The effect of the zero corner radius on the behavior of axially loaded fiber reinforced polymer (FRP) jacketed prismatic specimens has been studied experimentally by a number of researchers the majority of whom claims that a certain degree of effective confinement is provided by a jacket with sharp corners [19-21]. The experimental study of Wang and Wu [18], where 108 prismatic specimens were confined with FRP jackets with various corner radius, shed light on the influence of the corner radius on the strength and ductility increase. It was found that the strength gain of confined concrete columns, f_{cc}/f_{co} is in direct proportion to the corner radius ratio and independent of the confinement level and the concrete quality. Although no strength increase was observed in jacketed specimens with sharp corners, higher ductility levels were reached indicating the increased deformability ought to the provided confinement. Moreover, it was found that the attained ductility depends on both the concrete quality and corner of radius. Thus, for concrete quality C30/37 confinement is effective in increasing the ductility only in specimens with sharp or small corners, whereas for concrete quality C50/60 confinement is effective in increasing the ductility of all the column types.

The influence of the shape of the cross section on the effectiveness of the composite jackets is reflected through the confinement effectiveness coefficient [22]:

$$k_e = 1 - \frac{(b-2r)^2 + (h-2r)^2}{3A_g(1-\rho_l)} \tag{1}$$

where b, h are the width and height of the cross section, r is the corner radius, A_g is the cross sectional area and ρ_l is the percentage of the longitudinal reinforcement. The confinement effectiveness coefficient of the jacket becomes, k_e=1, for circular cross sections.

The lateral confining pressures induced by the FRP wrapping reinforcement on a rectangular cross section in the two principal directions are equal to [22]:

$$f_{lx} = \rho_{jx} k_e E_j \varepsilon_{ju} \text{ and } f_{ly} = \rho_{jy} k_e E_j \varepsilon_{ju} \tag{2}$$

where ρ_{jx}, ρ_{jy} are the volumetric ratios of the FRP jackets, k_e is the confinement effectiveness coefficient, E_j is the elastic modulus of the FRP wrap and ε_{ju} is the nominal deformation capacity of the jacket material. From Eqs. (1) and (2), it is evident the influence of the shape of the cross section on the provided lateral confining pressure.

All the above refer to the research that has been conducted so far on prismatic specimens wrapped with composite FRP jackets. The behavior of steel reinforced grout (SRG) jacketed prismatic specimens under compressive load is still under investigation. It is expected that the

corner radius is going influence the SRG jacketed members in the same way as in the FRP jacketed ones. In the test specimens presented herein, it was decided the sharp edges of the specimens to be left intact in order to simplify jacket construction.

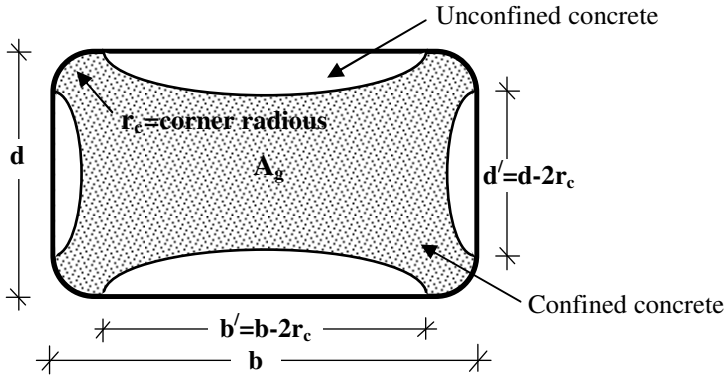

Figure 1: Confined core for rectangular cross sections.

2.2 Axial cyclic compression and its effect on confined concrete

The knowledge of the stress–strain behavior of concrete confined after wrapping with composite fabrics under cyclic compression is of particular interest in the seismic design of retrofitted structures as well as in performing nonlinear dynamic analysis. The majority of the experimental and analytical studies conducted so far focus on either FRP confined concrete cylinders or FRP confined specimens with rectangular cross section (concrete prisms) subjected to monotonic axial compression loading (e.g., [19]-[21],[23]-[25]). On contrary, the effect of axial cyclic compression on FRP confined specimens has been studied by a limited number of researchers (e.g., [26], [27]]. The research carried on FRP-confined concrete prisms is even more limited (e.g., [28]-[32]). Experimental evidence related to both unreinforced and reinforced FRP-confined specimens of various shapes and sizes subjected to different loading patterns (involving single or multiple complete unloading / reloading cycles at prescribed displacement levels, as well as partial loading / reloading cyclic loading) revealed the general trend which is that the envelope curves of cyclic stress–strain response are almost identical to the monotonic stress–strain responses of geometrically equivalent specimens.

The response of FRP-confined unreinforced prismatic specimens subjected to axial cyclic compression, was studied by Abbasnia and Ziaadiny [30], Abbasnia et al. [31, 32] with parameters of investigation the patterns of cyclic loading, the confinement level and the aspect ratio of the cross section. The main conclusions drawn are that: (i) the envelope curve of the cyclic stress-strain curve is similar to the monotonic stress-strain curve; (ii) plastic strain of FRP-confined concrete prisms is a linear function of the envelope unloading strain; (iii) unloading/reloading cycles have cumulative effect on the plastic strain and stress deterioration; (iv) the stress deterioration and plastic strain are independent of the column parameters; and (v) the unloading path is highly nonlinear and is dependant to the unconfined concrete strength. Moreover, it is commented by the authors that the effect of the sharpness of the section on the cyclic behavior of the FRP-confined prisms is an open issue that requires further research. Wang et al. [31] investigated the influence of axial cyclic compression to both reinforced and unreinforced square C-FRP confined columns. With test variables the section size, the volumetric ratio of hoop reinforcement, the number of layers of CFRP wrap and the damage level before CFRP wrapping, the square cross section columns were subjected to monotonic or cyclic axial loading. For one more time, it was observed that the envelope curves of

specimens subjected to cyclic loading were almost identical to the stress-strain responses of the monotonically loaded specimens. Other conclusions drawn are: (i) specimens subjected to cyclic axial compression attained larger axial strains compared to the monotonically loaded counterparts; (ii) failure of columns is postponed if subjected to unloading/reloading cycles; (iii) predamage had little effect on the monotonic stress-strain response; and (iv) the hoops provided influenced the ultimate axial strain capacities, the shape of the stress-strain curves and the shape of the unloading path and the plastic strains. Based on the results of their experimental campaign, Wang et al. [32] proposed an axial stress-strain model for C-FRP square reinforced confined RC columns which comprises a monotonic stress-strain model to describe the envelope curve, a polynomial expression for the unloading path and a straight line for the reloading path (Fig. 2).

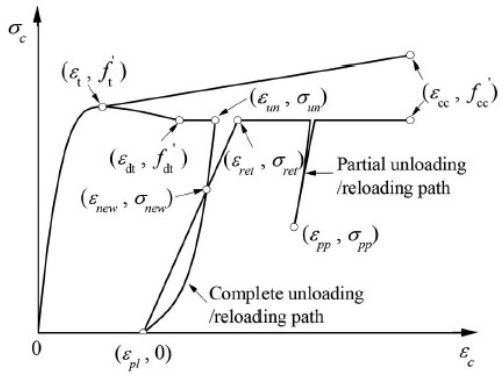

Figure 2: Schematic Cyclic stress-strain model proposed by Wang et al. [2].

3 EXPERIMENTAL PROGRAM

A number of unreinforced prismatic specimens with a 200-mm square cross section and a specimen height of 600 mm was tested in uni-axial compression (Fig. 3(a)). All specimens were wrapped with a single layer of steel fabric with the orientation of the high strength cords depicted in Fig. 3(b). The parameters considered in the investigation were: a) the density of the steel fabric and b) the rate of axial loading.

Two types of steel reinforced fabrics were used in the experimental program, the 3X2 and 12X (Fig. 3(c)). The 3X2 wire cord is made by twisting five individual wires together – three straight filaments wrapped by two filaments at a high twist angle, whereas the 12X wire cord is made by twisting two different individual wire diameters together in 12 strands with over twisting of one wire around the bundle. The density of the fabric related to the number and spacing of the steel cords was selected to be 2 cords/cm and 1 cord/cm, respectively, corresponding to medium and low density fabrics. The objective of utilizing fabrics of different type (12X and 3X2) and density (2 cords/cm, 1 cord/cm) was twofold. The different density aimed at investigating the influence of the fabric tensile strength on the provided lateral confining pressure, whereas the use of different types intended to examine whether the different surface roughness distribution has any effect on the quality of the interfacial mechanical interlock between the cords and cementitious grout matrix.

The rate of axial loading and its effect on the response of the steel grout jacketed specimens was another parameter of investigation. The specimens were subjected to monotonic concentric uni-axial compression load applied either in a slow rate reaching the maximum load in 400 sec or at a axial load rate ten times faster.

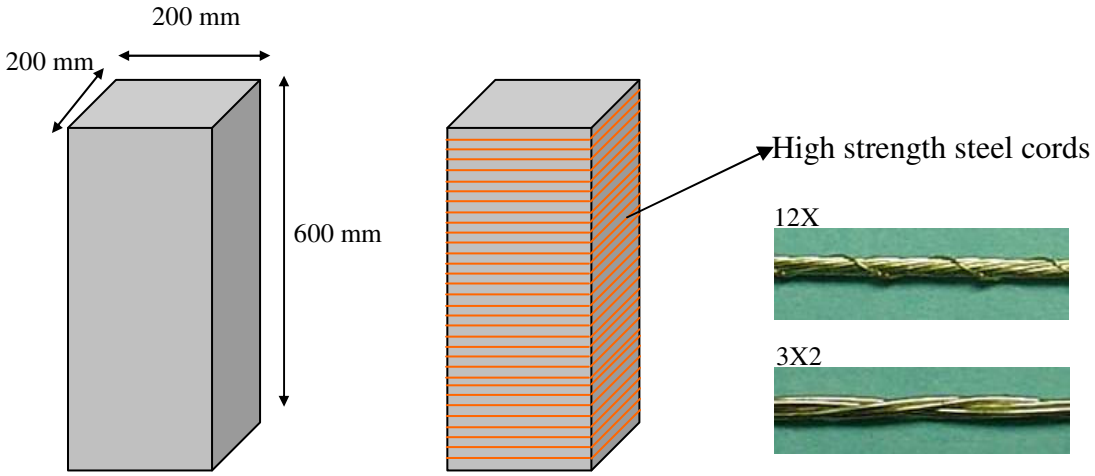

Figure 3: (a) Specimen geometry; (b) column wrapping – orientation of cords; (c) types of cords.

3.1 Test specimens

The number and characteristics of the test specimens appear in Table 1. Three prismatic specimens, No 1a, 13 and 14, were used as control specimens. With parameters the type of the steel fabric and its density four different jacket schemes are defined. Two of them were applied in the specimens of the current experimental study. The 3X2 low density steel reinforced fabric (1 cord/cm, i.e. spacing between successive cords 1 cm), named hereafter 3X2/1, was applied to specimens No 10 and No 12, whereas the 12X medium density fabric (2 cords/cm, i.e spacing between successive cords 5 mm), name hereafter 12X/0.5 cm, was applied to No 7, No 8 and No 9 specimens. In two of the jacketed specimens, No 7 and No 12, confinement was enhanced by the addition of an anchorage system placed at the end of the lap. Two load sequences were considered differentiated by the rate of the applied load and the inclusion or not of load/unload cycles. The slow rate loading, denoted as *slow* in Table 1, was applied at approximately 400 secs to specimens No 13, No 14 (unconfined) and No 9 (confined). The fast rate loading which included three load/unload cycles at two levels of the maximum axial load attained (a detailed description in provided in section 3), was applied 10 times faster to specimens No 1a (unconfined), No 7, No 8, No 10 and No 12 (confined).

Specimen ID	SRP type	Density (cords/cm)	Anchoring	Load type
1a	Control	Without confinement	No	fast
13	Control	Without confinement	No	slow
14	Control	Without confinement	No	slow
7	12X	2	Yes	fast
8	12X	2	No	fast
9	12X	2	No	slow
10	3X2	1	No	fast
12	3X2	1	Yes	fast

Table 1: Specimen details.

3.2 Material properties

The prismatic specimens were cast in one batch using concrete of moderate compressive strength classified as C25/30 (EC2, 2004). The concrete compressive strength defined by three cubes of 200 mm was 36 MPa. Both top and bottom surface of the specimens were

capped with a self-leveling high-strength mortar in order to ensure smooth surface for uniform loading.

The two types of high carbon steel cords, 3X2 and 12X, utilized in the experimental program had a micro-fine brass also known as AOBrass (adhesion optimised) coating. The tape density of the original 3X2 and 12X steel reinforced fabrics, as produced by the manufacturer, was 9.06 cords/cm considered high-density tape (Fig. 4(a)). The modified density of both the 3X2 and 12X consisted of 1 and 2 cords/cm characterized herein as low and medium density, respectively (Fig. 4(b)). Redundant cords were removed manually, paying attention not to damage the underlying net that essentially keeps the cords in position. The distance of 1.0 and 0.5 cm between successive cords in the low and medium density was considered satisfactory for uninhibited flow of the cementitious grout through the steel reinforced fabric. The mechanical properties of the steel reinforced fabrics used in the experimental study are presented in Table 2. The axial stiffness of the two types of fabric used for wrapping the prismatic specimens are: i) for 3X2/1 $K_f^{3X2/1}$=7320 N/mm and (ii) for 12X/2 $K_f^{12X/0.5}$=13158 N/mm.

Steel fabric type	Density (cords/cm)	Tape tensile load (N/cm)	Equivalent tape thickness (mm)	Tape stress (MPa)
12X	1	1250	0.062	2013.8
	2	2500	0.124	2013.8
3X2	1	1539	0.062	2479.4
	2	3078	0.124	2479.4

Table 2: Tape properties of the steel fabric types utilized in the experimental program.

A commercial cementitious grout with fibres and special additives was utilized as a binding material for the application of the SRP jackets. The mechanical characteristics at 28 days according to the manufacturer are flexural strength 6.78 MPa, compressive strength 22.1 MPa and adhesion to dry concrete 1.88 MPa.

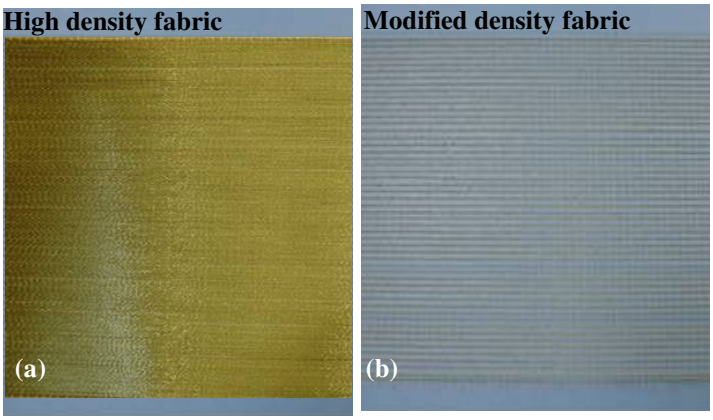

Figure 4: Steel reinforced fabric of (a) high and (b) modified density.

3.3 SRG wrapping

The first step of the proposed jacketing device comprised the application of a thin layer (≈0.5 cm) of cementitious grout placed manually with the help of a trowel directly onto the lateral surfaces of the prismatic member (Fig. 5(a)). The application of the steel fabric followed. In order for the fabric to be embedded in the connecting matrix, the grout was squeezed out between the rovings of the fabric by applying pressure manually (Fig. 5(b)). The

fabric was applied to one full-cycle with an overlapping length equal to the length of the side of the prismatic member (Fig. 5(c)). A final coat of the cementitious grout was applied to the exposed surface (Fig. 5(d)). The thickness of the grout layer including the steel fabric was only 10 mm thick.

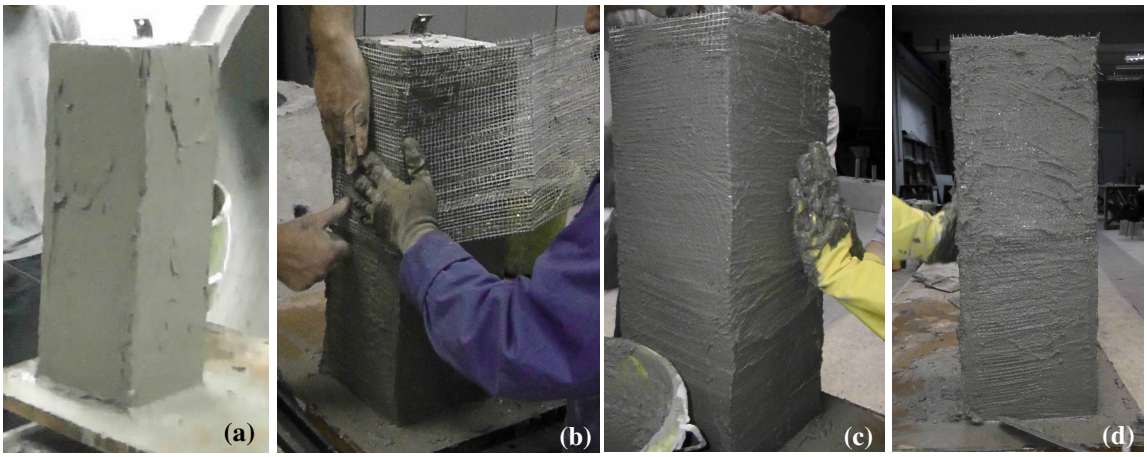

Figure 5: Application of the SRG jacket.

3.4 Confinement enhancement by the addition of an anchoring device

The previously described confinement schemes were selectively enhanced by adding the anchorage system depicted in Figs. 6(a), (b) (see Table 1). The scope behind the use of this anchoring scheme was to prevent sliding of the steel fabric from the end of the lap. Despite the fact that this was considered a probable mode of failure, it was not observed. Instead tensile fracture of the high strength steel cords at the corners of the prismatic specimens was the prevalent mode of failure . This justifies why the use of the anchorage system did no have any effect on the observed compressive strength as shown by experimental evidence (section 5).

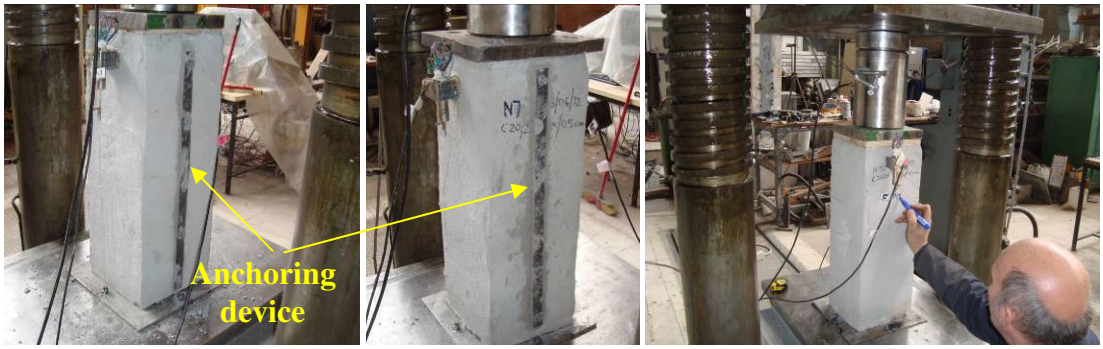

Figure 6: (a), (b) Confined specimens that include the applied anchoring; (c) Loading arrangement of the specimens placed at the loading machine.

4 INSTRUMENTATION AND LOADING ARRANGEMENT

The prismatic specimens were loaded till failure by using a compression testing machine of 6000 kN capacity. Specimens placed on the steel platform of the loading machine in such a way that the compressive load was applied along their central axis (Fig. 6(c)). The two end platforms of this loading machine are linked in a hinge manner in order to prohibit the development of moments at the end of the specimens. The applied axial compressive load was monitored by using a 5000 kN capacity load cell placed above the specimens, whereas verti-

cal deformations measured by using four linear variable displacement transducers (LVDTs) mounted at each side at the mid-height of the column. The axial compressive strain (shortening) of the specimen was found from averaging these vertical deformations and assuming a uniform distribution over the height of the specimen. The axial compressive stress value that corresponds to an axial load level was found by assuming uniform distribution of the axial compressive stress in the horizontal cross section of the specimen.

Two distinct types of loading sequences were applied. As far as the first loading sequence is concerned, the load was applied monotonically up to failure in a relatively slow rate reaching its highest value at approximately 400 seconds. In the second loading sequence an axial compressive load was again applied; however, this time three load-unload cycles were introduced in two levels of the axial load which corresponds to approximately 1/2 and 2/3 of the maximum load attained. These six load-unload cycles were followed with a final monotonic load increase up to failure of the specimen. The second loading sequence was applied at a relatively fast loading rate so that the six load-unload cycles together with the final loading up to failure took approximately 40 seconds being 10 times faster than the first loading sequence. With the available testing machine this was the fastest loading rate that could be possibly applied. This second sequence of load-unload cycles that are combined with a relatively faster rate of loading than the conventional slow-rate monotonic load termed herein as *fast* load simulates in laboratory conditions the axial compressive loads applied in a dynamic manner at vertical structural members located at the low levels of multi-story structures. Such loads resulting from the overturning mode of response due to the horizontal seismic forces are considered as additional axial loads to the axial loads resulting from other actions.

5 DISCUSSION OF OBTAINED RESULTS

In what follows the obtained results are presented in plots that depict for each tested specimen the variation of the applied load in terms of axial compressive stress together with the corresponding variation of the deformation of each specimen in terms of corresponding strain values reflecting the vertical shortening of each specimen.

The following parameters are examined:

(a) The effect of the loading rate; i.e. the effect of the two loading sequences described previously.

(b) The effect of the confinement for the two distinct schemes of confinement; namely 3x2/1 and 12X/0.5.

5.1 Effect of loading rate on unconfined concrete prisms

Figure 7 depicts the axial compressive stress – axial strain curves as obtained from three unconfined (No1a No13 and No14) concrete prismatic specimens. Two of the specimens (No13 and No14) were subjected to monotonically increasing axial load without any load-unload cycles adopting the conventional slow rate. The third specimen was subjected to the fast load sequence with the characteristics described in the previous section (i.e. the load was applied 10 times faster compared to specimens No13 and No14 and three load-unload cycles were introduced at two levels of the axial stress).

The average maximum compressive stress specimens No 13, No 14 loaded with the slow load rate was found equal to 31.1 MPa whereas the corresponding value for specimen No1b loaded with the fast load rate was found equal to 27.76 MPa, presenting a decrease of approximately 11%. Thus, it seems that the fast load sequence leads to a slight decrease in the axial

compressive strength but to an improved level of ductility. The modes of failure for the two types of loading are depicted in Fig. 8.

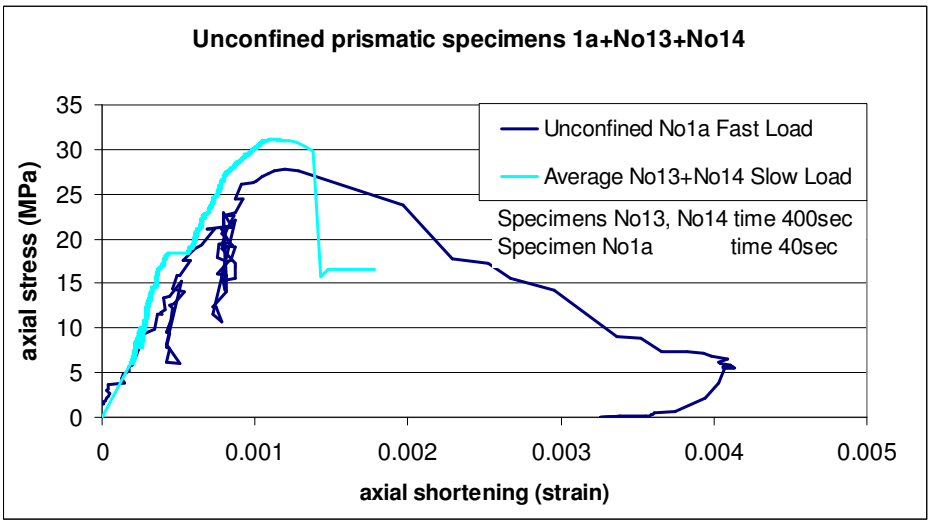

Figure 7: Comparison of axial stress – axial strain curves for the unconfined prismatic specimens subjected to the *fast* and *slow* loading sequences.

Figure 8: Mode of failure of unconfined specimens No 1a (fast loading rate) and No 13, No 14 (slow loading rate).

5.2 Effect loading rate on SRG confined concrete prisms

In Fig. 9 the response of two confined prismatic specimens (No10 and No12) subjected to the fast loading sequence are compared to the response of the unconfined prismatic specimens presented in the preceding section (No 1b, No 13, No 14). Both No 10 and No 12 specimens were confined by using the low density 3X2 steel fabric (1 cord/cm, see Table 1). The confinement of specimen No 12 was further enhanced by employing an anchoring scheme which aimed at delaying sliding of the steel fabric from the end of the lap (Fig. 4(a), (b)). The maximum axial compressive stress attained for specimen No 10 was equal to 30.85 MPa, whereas in the case of specimen No 12 a higher value was reached equal to 33.80 MPa due to the addition of the confinement device. These values represent an increase of 21.8% and 11.1% respectively, when they are compared to the corresponding maximum axial compressive stress value (27.76MPa) of the unconfined specimen No1a loaded with the same fast load rate conditions as the confined specimens.

From the above, it is evident that the steel fabric jacketing alone (without anchoring system) has a relatively small effect on the increase of the axial compressive strength when compared to that of the unconfined specimens (11.1% increase). The use of a simple anchoring scheme as in the case of specimen No 12 doubles the increase of the axial compressive strength of the jacketed specimens as compared to the corresponding one of the unconfined specimens (21.8% increase). Moreover, if the maximum compressive stress of the simple confinement specimen No 10 under fast loading rate (30.8 5MPa) is compared with that of the unconfined specimen (31.1 MPa) under slow loading rate (average of specimen No13 and No14) it is concluded that the low density steel fabric jackets (3X2, 1 cord/cm) cannot fully compensate for the loss of strength due to the relatively fast application of the load.

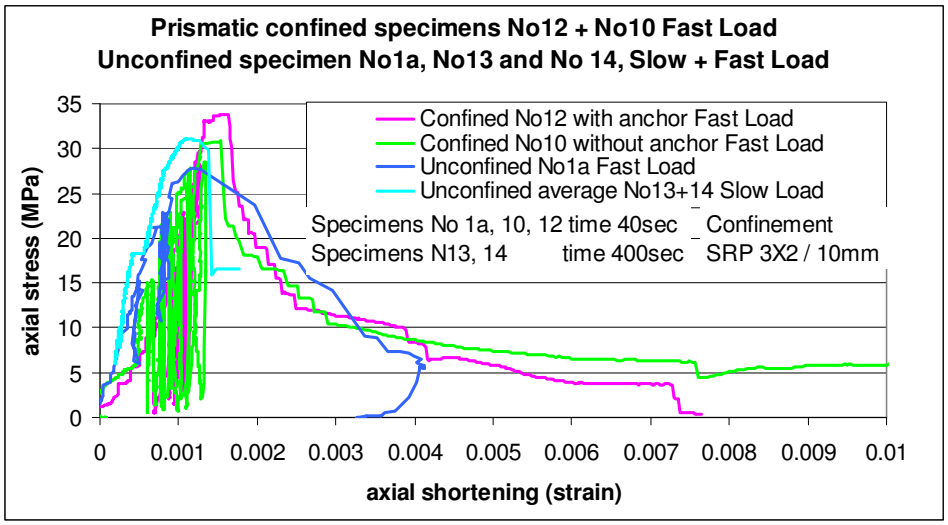

Figure 9: Comparison of axial stress – axial strain curves of the confined prismatic specimens No 10 and No12 to the unconfined prismatic specimens No 1a, No 13 and No 14 subjected to the *fast* and *slow* loading sequences.

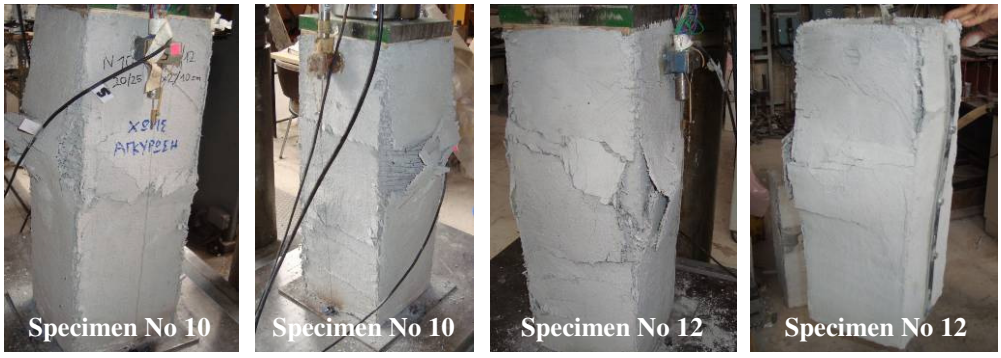

Figure 10: Mode of failure of confined specimens No 10 (without anchor, fast Load) and No 12 (with anchor, fast Load).

Figure 11 depicts the axial stress – axial strain response curves of specimens No 7, No 8 and No 9, which were all jacketed by employing the medium density 12X steel fabric (2 cords/cm, Table 1). The confinement of Specimen No 7 was further enhanced by employing the anchorage system presented in Figs. 4(a), (b). Specimens No 7 and No 8 were subjected to the fast loading rate, whereas specimen No 9 was subjected to the slow loading rate.

The comparison of the maximum axial compressive stresses attained for specimens No 7 (27.1 MPa) and No 8 (28.5 MPa) reveals that the anchorage system placed in specimen No 7 did not have any effect in increasing its maximum compressive strength (both specimens were subjected to the fast loading rate). At the same time specimen No 9 (simple confinement but loaded with the slow loading rate) reached a compressive strength equal to 36.41 MPa. Thus, for the 12X medium density jackets (2 cords/cm) a decrease of at least 21.7% of the maximum compressive strength can be attributed to the fast rate of loading (comparison between the maximum axial stresses attained by No 8 and No 9).

This decrease is twice as much as the corresponding decrease that was observed by comparing the obtained compressive strength of unconfined specimens No1b (27.76 MPa, fast load) and No13, No14 (31.1 MPa, slow load) depicted in Fig. 7. This is also shown in Fig. 13 where the obtained stress - strain response curves of confined specimens No 7, No 8 and No 9 are compared to the corresponding ones for the unconfined specimens No 1b, No 13 and No 14.

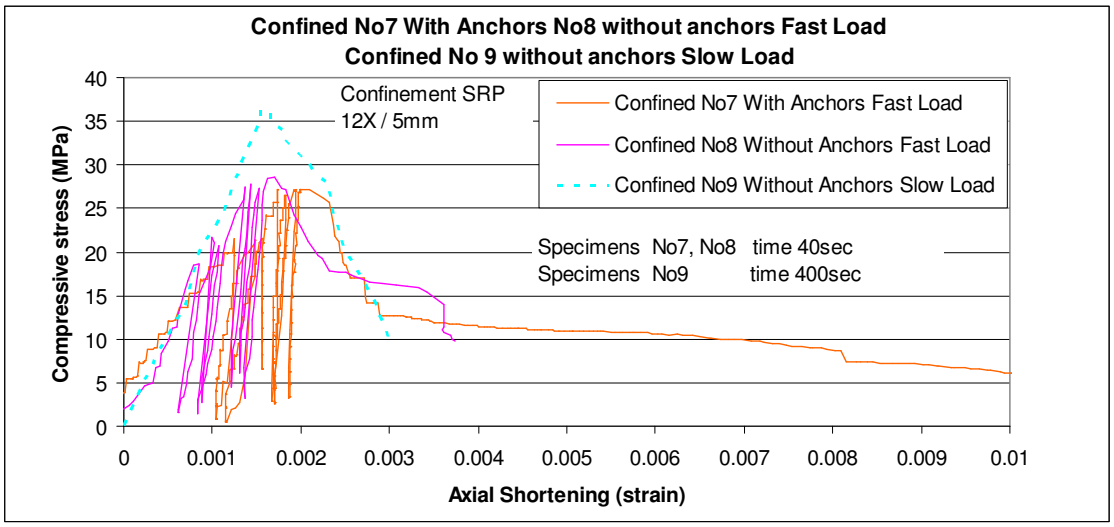

Figure 11. Comparison of axial stress – axial strain curves of the confined prismatic specimens No 7, No 8 and No 9 subjected to the *fast* and *slow* loading sequences.

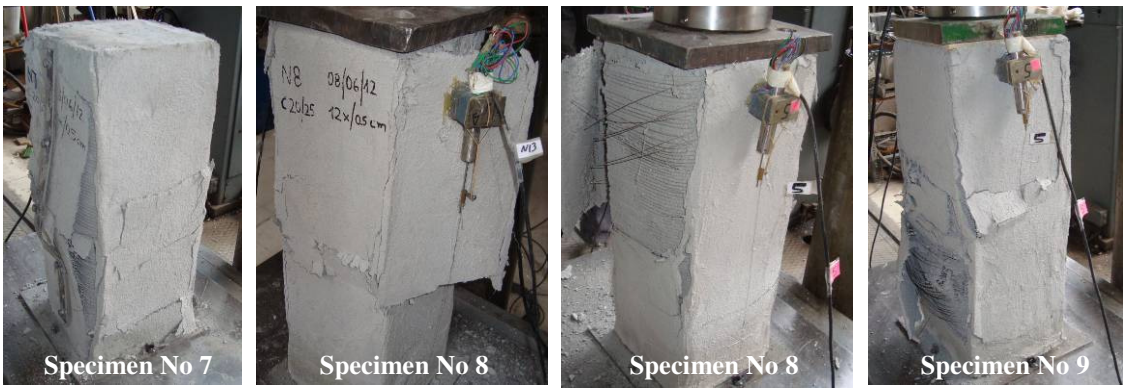

Figure 12: Mode of failure of confined specimens No 7 (with anchor, fast load), No 8 (without anchor, fast load) and No 9 (without anchor, slow load).

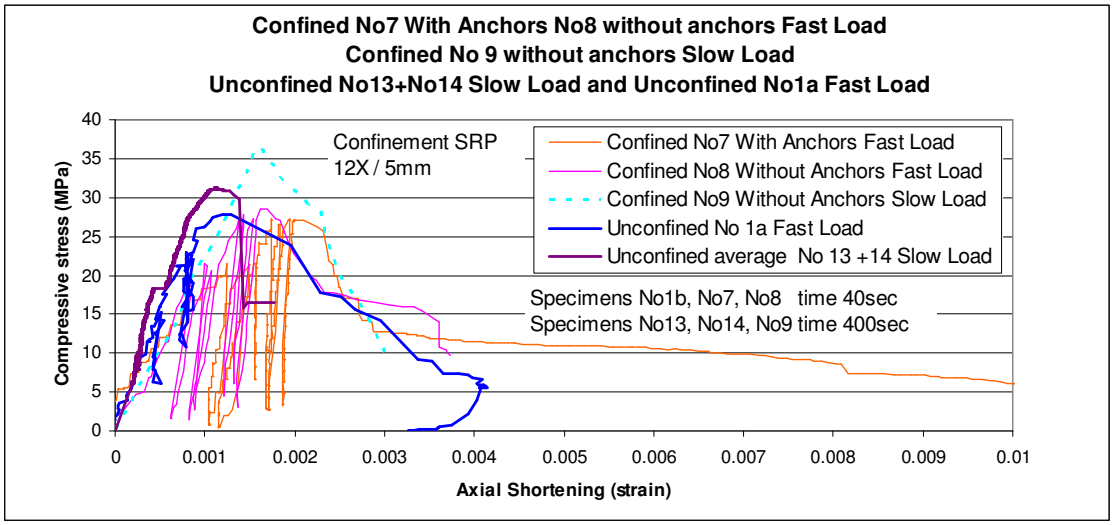

Figure 13. Comparison of axial stress – axial strain curves of the confined prismatic specimens No 7, No 8 and No 9 and the unconfined specimens No 1b, No 13 and No 14subjected to the *fast* and *slow* loading sequences.

6 CONCLUSIONS

The behavior of steel reinforced grout (SRG) jacketed concrete prisms subjected to both monotonic and cyclic axial loading was investigated experimentally. A single layer of steel reinforced fabric was applied to all specimens. Alternative jacketing schemes were applied depending on the density and the type of the fabric. The uni-axial compression load was applied to either a slow rate reaching the maximum load in 400 secs or at an axial load rate ten times faster. Despite the relatively small number of specimens used in the present investigation the following general conclusions can be drawn:

1. The fast loading rate of the applied axial compressive load results in an 11% decrease of the obtained strength of unconfined prismatic specimens.
2. In case of the medium density 12X (12x/0.5) SRG jackets, the slow rate of loading demonstrates an increase in compressive strength of 17%, whereas the fast rate load render this confinement ineffective as the obtained compressive strength of the confined specimen is almost the same as that of the unconfined specimen.
3. The recorded compressive strength of the low density (3x2/1) SRG jacketed specimens subjected to the fast loading rate considering also the favorable effect of the anchoring system is 22% larger than the unconfined strength for the same loading rate but only 9% higher compared to the slow loading rate of the unconfined strength.
4. Despite the preliminary nature of all these results it is revealed that such a dynamic application of compressive loads can lead to significant strength decrease for the tested confinement schemes that can almost render them ineffective. This does not mean that such an adverse effect can be expected to result from the dynamic application of the compressive load to any confinement scheme. However, it is a problem that should be investigated further considering also the effect of the edge sharpness and the number of fabric layers in the case of the SRG jacketing technique.

7 ACKNOWLEDGEMENTS

The authors wish to thank Dr. V. Kourtidis and Mr. T. Koukouftopoulos for their assistance in the experimental program. The program was conducted in the Laboratory of Strength of Materials and Structures and funded by the Research Committee of Aristotle University of Thessaloniki within the frame work of the program "Funding for new researchers". The materials were donated by SIKA Hellas and Interbeton.

REFERENCES

[1] S. Kurtz, P. Balaguru, Comparison of inorganic and organic matrices for strengthening of RC Beams with carbon sheets. *ASCE Journal of Structural Engineering*, **127(1)**, 35-42, 2001.

[2] T.C. Triantafillou, C.G. Papanicolaou, P. Zissimopoulos, T. Laourdekis, Concrete confinement with textile-reinforced mortar jackets, *ACI Structural Journal*, **103(1)**, 28-37, 2006.

[3] B. Barton, E. Wobbe, L.R. Dharani, P. Silva, V. Birman, A. Nanni, T. Alkhrdaji, J.Thomas, G. Tunis, Characterization of reinforced concrete beams strengthened by steel reinforced polymer and grout (SRP and SRG) composites. *Materials science and engineering A*, **412** , 129–136, 2005.

[4] P. Casadei, A. Nanni, T. Alkhrdaji, J. Thomas, Performance of double-T prestressed concrete beams strengthened with steel reinforced polymer. *7th International Symposium on Fiber Reinforced Polymer Reinforcement for concrete structures*, Kansas, USA, Paper No. SP-230-44, 2005.

[5] W. Figeys, L. Schueremans, K. Brosens, D. Van Gemert, Strengthening of concrete structures using steel wire reinforced polymer. *7th International Symposium on Fiber Reinforced Polymer Reinforcement for concrete structures*, Kansas, USA, Paper No. SP-230-43, 2005.

[6] K. Katakalos, C.G. Papakonstantinou, Fatigue of reinforced concrete beams strengthened with steel-reinforced inorganic polymers. *ASCE Journal of Composites for Construction*, **13(2)**, 103-112, 2009.

[7] Y.J. Kim, A. Fam, M.F. Green, Flexural strengthening of reinforced concrete beams with steel-reinforced polymer composites: analytical and computational investigations. *Journal of reinforced plastics and composites*, **29(14)**, 2141-2155, 2010.

[8] Y.J. Kim, A. Fam, M.F. Green, Application of SRP composite sheets for retrofitting reinforced concrete beams: Cracking and tension stiffening. *Journal of reinforced plastics and composites*, **29(17)**, 2647-2662, 2010.

[9] Y.J. Kim, A. Fan, A. Kong, R. El-Hacha, Flexural strengthening of RC beams using steel reinforced polymer (SRP) composites. *7th International Symposium on Fiber Reinforced Polymer Reinforcement for concrete structures*, Kansas, USA, Paper No. SP-230-93, 2005.

[10] A. Lopez, N. Galati, T. Alkhrdaji, A. Nanni, Strengthening of a reinforced concrete bridge with externally bonded steel reinforced polymer (SRP). *Composites: Part B*, **8**, 429–436, 2007.

[11] M. Pecce, F. Ceroni, A. Prota, G. Manfredi, Response prediction of RC beams externally bonded with steel-reinforced polymers. *ASCE Journal of Composites for Construction*, **10(3)**, 195–203, 2006.

[12] A. Prota, Tan K.-Y., A. Nanni, M. Pecce, G. Manfredi, Performance of shallow reinforced concrete beams with externally bonded steel-reinforced polymer. *ACI Structural Journal*, **163(2)**, 163-170, 2006.

[13] G.J. Mitolidis, T.N. Salonikios, A.J. Kappos, Tests on RC beams strengthened at the span with externally bonded polymers reinforced with carbon or steel fibers. *ASCE Journal of Composites for Construction*, **16(5)**, 2012.

[14] G.E. Thermou, S.J. Pantazopoulou, Metallic fabric jackets: an innovative method for seismic retrofitting of substandard RC prismatic members. *Structural Concrete Journal***,** The fib Journal, Thomas Telford, **8(1)**, 35-46, 2007.

[15] R. El-Hacha, K. Abdelrahman, Slenderness effect of circular concrete specimens confined with SFRP sheets. *Composites: Part B*, **44,** 152–166, 2013.

[16] R. El-Hacha, M.A. Mashrik, Effect of SFRP confinement on circular and square concrete columns. *Engineering Structures*, **36,** 379–393, 2012.

[17] G.E. Thermou, Concrete confinement through a novel intervention scheme, the steel reinforced grout jackets. *Workshop of the Hellenic Society of Civil Engineering* "The seismic engineering through the scientific approach of young researchers and engineers", Thessaloniki, Greece (in Greek), 2012.

[18] Y.A. Al-Salloum, Influence of edge sharpness on the strength of square concrete columns confined with FRP composite laminates. Composites: Part B, 38, 640–650, 2007.

[19] P. Rochette, P.Labossiere, Axial testing of rectangular column models confined with composites. ASCE Journal of Composites for Construction, 4(3),129–136, 2000.

[20] O. Chaallal, M. Hassan, M. Shahawy, Confinement model for axially loaded short rectangular columns strengthened with fiber-reinforced polymer wrapping. *ACI Structural Journal*, **100(2)**, 215–221, 2003.

[21] L.-M. Wang, Y.-F. Wu. Effect of corner radius on the performance of CFRP-confined square concrete columns: Test. *Engineering Structures*, **30,** 493–505, 2008.

[22] fib Bulletin 14, Externally Bonded FRP Reinforcement for R.C. Structures. *Report by Task Group 9.3*, federation international du béton (fib), Lausanne Switzerland, 130, 2001.

[23] A. Mirmiran, M. Shahawy, M. Samaan, H.E. El-Echary, J.C. Mastrapa, O. Pico, Effect of column parameters on FRP-confined concrete. *ASCE Journal of Composites for Construction*, **2(4)**, 175–185, 1998.

[24] S.T. Smith, S.J. Kim, H.W. Zhang, Behavior and effectiveness of FRP wrap in the confinement of large concrete cylinders. *ASCE Journal of Composites for Construction*, **14(5)**, 573–582, 2010.

[25] Y. Xiao, H. Wu, Compressive behavior of concrete confined by carbon fiber composite jackets. ASCE Journal of Materials in Civil Engineering, **12(2)**, 139–146, 2000.

[26] L. Lam, J.G. Teng, C.H. Cheng, Y. Xiao, FRP-confined concrete under axial cyclic compression. Cement and Concrete Research, **28(10)**, 949–958, 2006.

[27] T. Ozbakkaloglu, E. Akin, Behavior of FRP-confined normal- and high-strength concrete under cyclic axial compression. *ASCE Journal of Composites for Constr*uction, **16(4)**, 451-463, 2012.

[28] R. Abbasnia, H. Ziaadiny, Behavior of concrete prisms confined with FRP composites under axial cyclic compression. *Engineering Structures*, **32**, 648-655, 2010.

[29] R. Abbasnia, R. Ahmadi, H. Ziaadiny, Effect of confinement level, aspect ratio and concrete strength on the cyclic stress–strain behavior of FRP-confined concrete prisms. *Composites: Part B*, **43,** 825–831, 2012.

[30] R. Abbasnia, F. Hosseinpour, M. Rostamian, H. Ziaadiny, Cyclic and monotonic behavior of FRP confined concrete rectangular prisms with different aspect ratios. *Construction and Building Materials*, **40**, 118–125, 2013.

[31] Z. Wang, D. Wang, S.T. Smith, D. Lu, CFRP-confined square RC columns. I: Experimental investigation. *ASCE Journal of Composites for Construction*, **16(2)**, 150-160, 2012.

[32] Z. Wang, D. Wang, S.T. Smith, D. Lu, CFRP-confined square RC columns. II: Cyclic axial compression stress-strain model. *ASCE Journal of Composites for Construction*, **16(2)**, 161-170, 2012.